International Journal of Geosciences, 2025, 16(9), 658-671
https://www.scirp.org/journal/ijg
ISSN Online: 2156-8367
ISSN Print: 2156-8359

Engineering Assessment of Umm al Khair Dam (Jeddah, Saudi Arabia)

Marwan Al Saikhan

Applied Geology Center, Saudi Geological Survey, Jeddah, Saudi Arabia
Email: alsaikhan.marwan@gmail.com, saikhan.mm@sgs.gov.sa

How to cite this paper: Al Saikhan, M. (2025) Engineering Assessment of Umm al Khair Dam (Jeddah, Saudi Arabia). *International Journal of Geosciences*, **16**, 658-671.
https://doi.org/10.4236/ijg.2025.169032

Received: June 28, 2025
Accepted: September 26, 2025
Published: September 29, 2025

Abstract

Jeddah is the second-largest city in Saudi Arabia, with a population of 3 million. A large earthfill dam was constructed in 2012 to mitigate flash-flood hazards from Wadi Mthawab, following the catastrophic events of 2009 and 2011. An extensive evaluation was carried out to verify the capacity and stability of this dam. The study includes hydrology and geotechnical analyses. The flood for 300 and 500 years return periods was predicted from local IDF curves. The obtained peak discharge (Qp) and runoff volume (Vh) for T300 and T500 are 207 m^3/s and 224 m^3/s respectively; the equivalent Vh are 3.3×10 m^3 and 3.5×10 m^3. The dam's static stability was assessed against overturning, dam-face sliding and foundation bearing. The obtained factors of safety (Fs) using limit-equilibrium methods are 1.94, 1.32 and 1.8 respectively. The reservoir capacity is 3.5×103 m^3, and the dam outlet demonstrated its ability to discharge the reservoir water within a short time (36 hours). Wind-induced wave action was found to be negligible. Results confirm that the dam safely accommodates design floods up to the 500-year event without overtopping or stability compromise. It seems Umm al Khair Dam satisfies its design aim as flood mitigation and has proved that it is stable and can match a 500-year storm if continuous safety measures are reviewed. Continuous tracking of seepage, pore-pressure, and structural movement is advised to sustain long-term operation and safety.

Keywords

Jeddah, Umm al Khair Dam, Earthfill Dam, Flood, Wadi Bani Malik

1. Introduction

In 2009 and 2011, Jeddah suffered from two devastating floods that caused dozens of casualties and significant destruction. It was not due to heavy rain, but to the lack of proper flood protection. In 2012, the authorities conducted an extensive protection system that included more than 10 dams and numerous channels of different sizes. The earthfill dam under investigation (Umm al Kair), emerged as one of the most important, as it prevents the flood danger from the largest of these wadis, Wadi Mthawab. The dam site is located on the western side of the city (**Figure 1**), comprising hills and alluvial plains. The rocks in the catchment area and the reservoir are Precambrian schist, marble, meta-andesite, and metabasalt, intruded in many locations by diorite and quartz diorite (Moore & Al-Rehaili, 1989) [1]. The regional structures that affect the area are influenced by the Red Sea formation, with joints and minor faults that trend northwest (Al Shanti, 1966) [2]. Quaternary alluvial and eolian deposits cover the reservoir.

Figure 1. Location map of Umm al Khair earthfill dam and Wadi Mthawab catchment area, situated on the western side of Jeddah. The figure shows the surrounding hills, alluvial plains, and the general geomorphological setting that controls runoff into the reservoir.

Geologically, the area has been extensively studied by numerous researchers. Brown *et al.* [3] (1963) published the first reconnaissance 1:500,000-scale geological map for the southern Hijaz quadrangle. It was followed by more detailed studies of specified areas by AI-Shanti (1966), Nebert *et al.* (1974) [4], and Badokhon (1998). The limited information on subsurface conditions is summarized in the Engineering Geological Map of Jeddah by Laurent *et al.* (1973) [5]. Khogandi (1989) [6] reported more updated geology. The engineering geology of the Greater Jeddah metropolitan area encompasses the geotechnical properties of soil at both the surface and subsurface levels, as reported by Alqahtani (1998) [7].

The shape of the earthfill dam is sinuous, extending for 300 m. The dam is trapezoidal in cross-section, 9.5 m high at its maximum (from 41.5 to 50 m above sea level, a.s.l.), and the freeboard is 1.0 m. The crest is 8 m wide, and the slope of its two faces is 3H:1V (**Figure 2(a)**). The dam volume exceeds 200,000 m^3 and is composed of compacted silty sand mixed with gravel and cobbles. The water level behind the dam would reach 8.5 m during a heavy storm. The upstream face is covered by concrete slabs 10 cm thick, while the downstream face is protected by 40 cm thick riprap. The outlet pipes are 3 m in diameter, which cross the dam at the bottom; it is protected by trash racks (**Figure 2(b)**). The earthfill dam is draining downstream into a concrete channel with a trapezoidal shape, 724 m long and 8 m wide at the bottom, with a slope of 0.25%. The channel discharge capacity is 120 m^3/s (**Figure 2(c)**). It has a trapezoidal cross-section with a maximum height of 7 m and a 1.0 m freeboard. The dam is 8 m wide crest, with 3H:1V slopes on both faces (**Figure 3**).

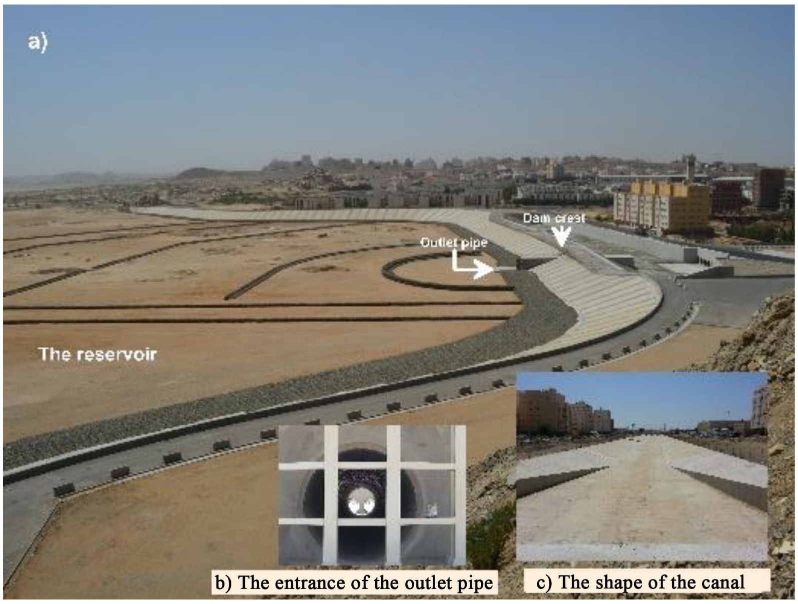

Figure 2. General views of the dam and its associated structures: (a) Cross-sectional geometry of the earthfill dam showing crest width, height, and slope ratios; (b) Entrance of the outlet pipe with protective trash rack designed to prevent debris blockage; (c) Concrete trapezoidal downstream canal extending 724 m, with a capacity of 120 m^3/s to safely convey floodwaters away from urban areas.

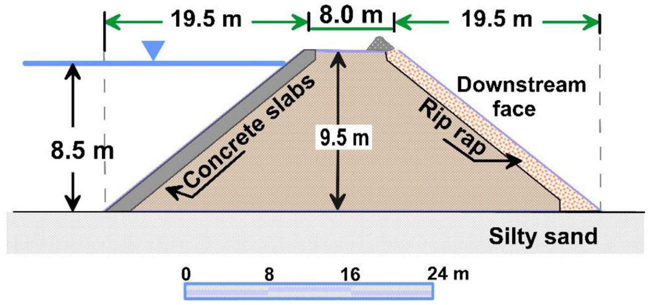

Figure 3. Detailed cross-section of the Umm al Khair dam showing dam body dimensions, crest width, freeboard, and protective layers (upstream concrete slabs and downstream rip rap).

The primary objective of this study is to assess the dam's ability to withstand the thrust of floodwaters and its capability to discharge the flood volumes corresponding to 100, 300, and 500-year recurrence intervals.

2. Flood Hazards

Geological hazard, in general, refers to any potentially dangerous process that affects the productive capacity and sustainability of a population. Flood and soil slope failure are typical examples of instability in the case of earthfill dams. The primary purpose of this earthfill dam is not to store water permanently, but to safely regulate the flow of flood water through a densely populated neighborhood downstream. Three factors control safe flood flow:

1) Dam reservoir capacity;
2) Flow rate through the dam outlet and;
3) Earthfill dam stability.

The dam reservoir and Wadi Mthawab watershed were delineated using the area Ladar map and WSM software. The original reservoir is flat, surrounded by moderately high hills, and has a capacity of approximately 3.5×10^3 m^3 (**Figure 4**).

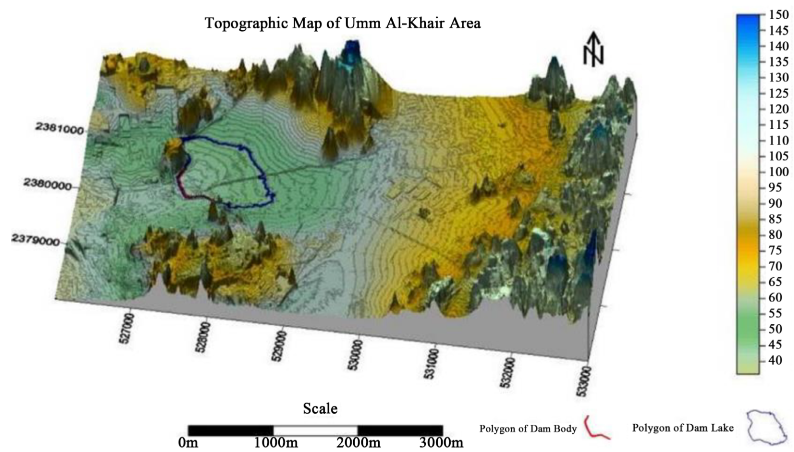

Figure 4. Relative size of Wadi Mthawab watershed compared to the reservoir area of Umm al Khair Dam. The delineated catchment boundaries highlight how runoff is concentrated into the storage basin during major storm events.

Hadadin *et al.* (2013) analyzed the unusual November 2009 flash flood, which occurred in Jeddah, resulting in 90 mm of rainfall in 24 hours. The estimated natural peak discharge is Qp = 160 m^3/s for a return period of 50 years (T_{50}) storm in Wadi Mthawab using the Snyder unit hydrograph. The estimated storm up of T_{100} is Qp = 177 m^3/s, with a runoff volume (V_h) of 2.83×10^3 m^3. Local Intensity-Duration-Frequency (IDF) curves were implemented, in this study, for a duration of 24 hours to determine design rainfall depths for T = 300 and 500-year storms. The obtained results were converted into rainfall depth versus time (hyetographs). These hyetographs were then applied to the Snyder unit-hydrograph parameters estimated by Hadadin *et al.* (2013) to induce design runoff hydrographs, from which Q_p and V_h can be obtained. The attained Qp and Vh values for T_{300} and T_{500} are presented in **Table 1**, which shows that the reservoir capacity is capable of accommodating the water volume up to the T_{500} level.

Table 1. The values of Qp and V_h with a duration of 24 hr for various return periods.

	Return Period, yr	Peak Discharge, m^3/s	hydrograph volume, m^3
1	100	177	2.83×10^3
2	300	207	3.30×10^3
3	500	224	3.50×10^3

The reservoir capacity at spillway level (50.2 m above sea level) is approximately 3.5×10^3, equivalent to a water level of 8.5 m behind the dam. With simple cross multiplication, the time required for a T_{500} flood to fill the reservoir to the level of the spillway is 1 hour and 40 minutes. Two pipes at the bottom of the dam are connected to a downstream channel; each pipe is 1 m in diameter. The flow rate through each pipe (Vr) is:

$$Vr = (2\ g\ h_1)\ 0.5$$

where g = acceleration gravity (9.8 m/s^2) and

h_1 = water height behind the dam (maximum level 8.5 m), hence

$$Vr = [2\ (9.8)\ 8.5]\ 0.5 = 12.9\ m^3/s.$$

This relatively high rate is due to the water column behind the dam (8.5 m). The water pressure will decrease to nearly zero when the water level is 1 m (the upper level of the pipe).

The time (t) required to empty the reservoir water is estimated as follows:

The upper part of the pipes (h_1) is 7 m above the ground, and the time in seconds (t) is:

$$t = \{2\ As\ [(h_1)\ 0.5 - (h_2)\ 0.5] / C\}$$

where As = the pipe cross-sectional area

d = the pipe diameter (1 m),

C = constant = 4.52

h_2 = reservoir lower water level

then for one pipe, t = 18 hour, or t = 36 hours for two pipes (1.5 days).

On the other hand, the effect of water waves is also considered here to prevent water splashing over the dam crest. The average wind speed in Jeddah is 30 km/hr but may reach 100 km/hr with severe storms in winter (November-March). Wind comes from the north-northwest direction, producing water waves that are 1 m high in the reservoir (Yesubabu *et al.*, 2016 [8]; Alsaaq and Shamji, 2022 [9]). Although the wind speed is relatively high, it blows toward the southeast, away from the dam, and does not pose a danger to the dam.

3. Engineering Geological Mapping

One of the aims of engineering geological studies is to describe and classify the surface earth materials (soil and rocks) and draw boundaries whenever there are changes in material types or a change in their engineering properties within the same material. The soil field description was carried out in two trenches, 3 m deep (TP 1 and TP 2), and the soil and rock description was carried out further in two boreholes, 20 m deep (BH 1 and BH 2) (**Figure 5**). The measured rock values in each rock station are compared to those of the adjacent one; any variation in any parameter will categorize the two stations into two different rock zones according to the system given by the Geological Society of London (1977) [10]. Likewise, the variation in any soil parameter makes that location an independent soil zone from the surrounding zones, as recommended by the IAEG (1976) [11].

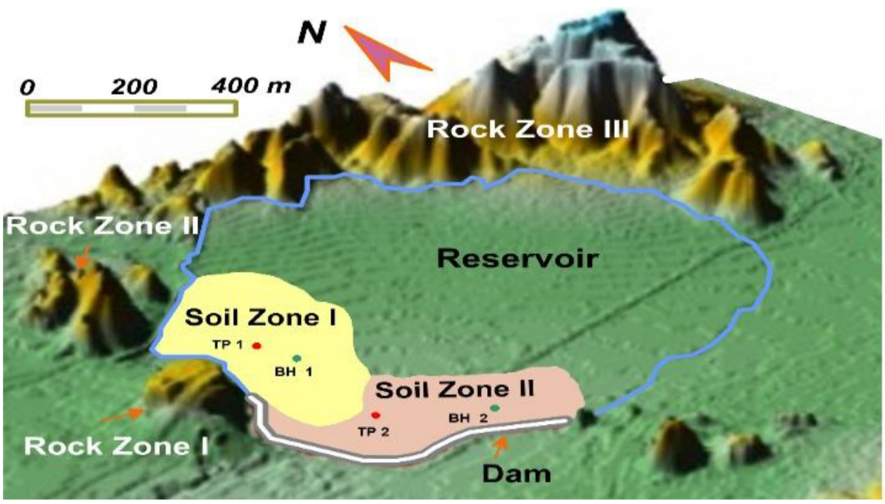

Figure 5. Engineering geological map of the dam site showing the spatial distribution of soil and rock zones. Soil zones are classified as silty sand (SM) and clayey sand (SC), while rock masses are categorized by Rock Mass Rating (RMR) values, indicating variations in strength, weathering, and fracture spacing across the foundation and abutments.

According to the Unified Soil Classification System, the area is composed of two soil types: silty sand (SM), which is a widespread soil in Jeddah, and clayey sand (SC). The soils were described in terms of grain color, shape, size, gradation, and surface roughness (IAEG, 1979) as follows:

Zone I*: *Silty sand with gravel

The silty sand (SM) is light brown and is primarily located along the dam's width. The grain's shape is subrounded to rounded. The water flow in the catchment area is slow, as influenced by the gentle slope in the studied area.

Zone II*: *Clayey sand with gravel

The color of the clayey sand (SC) is light brown, and the sand grains are mixed with gravel in some places. The grain shapes are subrounded. The soil is restricted to a relatively small, low-lying area southwest of the dam abutment, where the water flow is very slow.

The rocks were grouped according to the Rock Mass Rating (RMR) classification system. Rock description was based on rock weathering (W), strength (S), fracture spacing (F), and RQD (R). The essence is to transfer these measurements and descriptions into quantitative values or ranges by using some standard tables and charts.

The collective rock descriptive terms in each of the three stations are as follows:

***Zone I*: Andesite: (W2.S1.F2.R3)**

The rock mass in this zone is described as a slightly weathered (**W2**), extremely strong rock (**S1**), widely spaced fractured (**F2**), Fair RQD (**R3**).

***Zone II*: Andesite: (W3.S2.F4.R3)**

The rock mass in this zone is described as a moderately weathered (**W3**), very strong rock (**S2**), closely spaced fractured (**F4**), Fair RQD(**R3**).

***Zone III*: Andesite: (W3.S4.F5.R5)**

The rock mass in this zone is described as a moderately weathered (**W3**), moderately strong rock (**S4**), very closely spaced fractured (**F5**), very poor RQD (**R5**).

The spatial distribution of the rock and soil zones is presented in **Figure 5**.

4. Dam Stability

The procedure of dam stability is based on thorough regulations established individually by the Bureau of Reclamation (USBR), the U.S. Federal Energy Regulatory Commission (FERC) [12], and the U.S. Army Corps of Engineers (USACE) [13]. Their engineering processes follow the limit equilibrium analysis. Dam stability will be evaluated against the static force of the reservoir water. The dam cross-sectional area is demonstrated in **Figure 6**. When the dam reservoir is full, it will be subjected to three forces: (1) a lateral load that is imposed on the dam slopes, (2) an uplift pressure underneath the dam, and (3) the water table within the embankment may be raised, possibly lowering the soil shear strength. The stability of the dam slopes is controlled by several factors related to embankment geometry, as well as geological and hydrogeological factors (Zhou *et al.*, 2023 [14], **Table 2**). A combined effect of these factors may determine failure conditions along the weak surface, making the movement of a specific soil volume kinematically possible. Water tightness and the prevention of seepage are closely related to the dam's purpose and, at the same time, to dam stability.

Table 2. Factors that affect earthfill dam stability.

1	Slope geometry (slope angle and height)
2	Soil shear strength (cohesion and friction angle)
3	Reservoir water level (lateral water pressure)
4	Internal Pore-water pressure and drainage
5	Foundation conditions
6	Wind speed and height

In this study, the static stability of dams is analyzed for three failure types:

- Foundation bearing capacity (USACE EM 1110-2-1902, 2003)
- Dam overturning (Fell *et al.*, 2014) [15]
- Upstream face stability (USBR DS-13 §4, 2011)

The dam was founded on alluvium, which is composed mainly of sand mixed with silt and cobbles. The soil density is 2 t/m^3, and the load of 8.5 m (from dam crest to base) on the foundation is 17 t/m^2. (167 kN/m^2). The SPT N-value ranges from 8 (loose) to 30 (medium dense). If N = 15 is considered, then the foundation can support a stress of more than 300 kPa (Das, 2018) [16], with a factor of safety (Fs) of 1.8.

The dam is subjected to a horizontal water load and a vertical force underneath; its stability relies on the body weight acting vertically and is considered a positive force. Since the forces are acting in different directions, the moments around the dam toe of each force were calculated individually, and their combined effect was summed algebraically to predict the factor of safety (Fs). From simple trigonometry, using the dam's dimensions, the dam's cross-sectional area is 193 m^2. Accordingly, the weight of the dam with a meter width is 386 t. This force is acting downward and located in the dam's center of gravity (**Figure 6**), its moment for an arm of 19.5 is:

$$(Wt) = 386 \times 19.5 = 7{,}527$$

The water stored in the reservoir creates horizontal forces (Fw) on the upstream side of the dam that gradually increase with water depth (h). The resultant of the water pressure on the dam face is acting at a height of h/3 and is given by the Equation:

$$Fw = 0.5\ \gamma w\ (h)^2 = 24.5\ t/m^2$$

Where γw = water density (1.0 t/m^3)

h = the desired water level in the reservoir (h = 7 m).

The negative lateral pressure for an arm of 2.33 m is 57 t/m^2.

The dam base (B) equals 40.5 m (**Figure 6**), the numerical U-value per unit dam length can be calculated by:

$$U = 0.5\ \gamma_w\ B\ h = 141.8$$

The negative uplift moment for an arm of 27 m is 3,828. **Table 2** presents the results of dam stability and factor of safety. **Table 3** presents the results of dam stability and factor of safety.

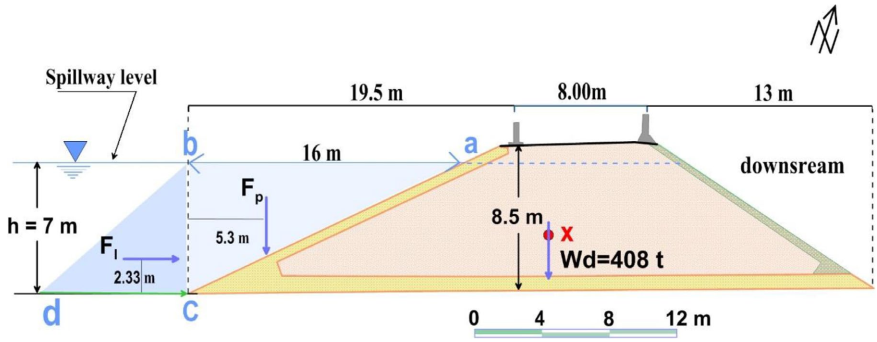

Figure 6. Schematic representation of forces acting on the dam cross-section when the reservoir is full. The diagram shows dam weight, hydrostatic pressure on the upstream face, and uplift pressure at the base, which were used to calculate moments and factors of safety against overturning and sliding.

Table 3. Summary of the acting forces, their moments and dam factor of safety (Fs).

	Force magnitude	Moment arm (m)	Moment	
Dam weight	386	19.5	+7,527	Total positive moments = +7,527 Total negative moments = +3,885.1 Fs = 1.94
Water lateral force	24.5	2.33	−57.1	
Water uplift	141.8	27	−3,828	

5. Upstream Face Stability

The stability of the dam's upstream inclined face is commonly evaluated using the limit equilibrium method (Terzaghi *et al.*, 1996) [17]. Gravity is a driving force that tends to move the face downward, and failure will occur if the soil strength does not have enough resistance and the factor of safety (Fs) is:

$$\text{Fs} = \frac{\text{Forcess resisting slide}}{\text{Forcess tending to slide}}$$

If a slice of the soil slope with a friction angle (φ) is considered (**Figure 7**), then the driving force (Fd) along the slip surface will be resisted by the soil strength. Depending on the face inclination (β), the driving force (Fd) having a certain weight (W) is:

Fd = W sin **β**

The Fd-value can be resolved into N and Fr as follows (**Figure 7**):

Fr = N tan

N = W cos **β**

then

$$Fs = \frac{Fr}{Fd} = \frac{N\tan\varphi}{W\sin\beta} = \frac{W\cos\beta\tan\varphi}{W\sin\beta}$$

Since $\frac{\cos\beta}{\sin\beta}$ in the last term is equal to $\tan\beta$, then,

$$Fs = \frac{\tan\varphi}{\tan\beta}$$

Based on the dam description, the dam slopes β-value is 18.43 and the minimum angle of friction is 30˚; hence, the safety factor of Umm al Khair dam is:

$$Fs = \frac{\tan 30}{\tan 23.55} = \frac{0.5774}{0.3332} = 1.32$$

The Fs value for Umm al Khair dam is adequate.

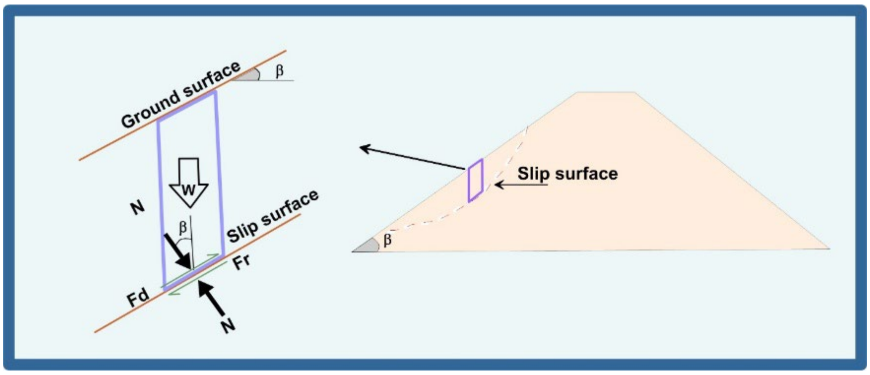

Figure 7. Stability analysis of the upstream slope using the limit equilibrium method. The diagram illustrates the relationship between driving and resisting forces along a potential slip surface, as well as the role of slope angle (β) and soil friction angle (φ) in determining the factor of safety.

6. Rock Slope Stability

Rock slope stability is an important part of assessing dam safety; slope failure in large blocks generates water waves that may overtop the dam. Zone 1 is the closest cliff, which represents the northern dam shoulder. It is 40 m high and extends for 330 m. The slope face is dipping 84˚ toward a 250˚ direction. Approximately 100 joint readings of random measurements of dip and dip direction were performed. The joints are naturally clustered into three sets, with the following averages: 89/175, 76/252, and 85/283.

The Dips 7 program was used to perform the rock kinematic analysis, checking the possibilities of plane and/or wedge failure. The size of plane failures ranges from a few cubic meters to large-scale landslides. Wedge failure is more frequent than plane failure, and its formation and occurrence depend primarily on the lithology and structure of the rock mass (Piteau, 1972) [18]. Wedge failures occur along two joints from different joint sets whose intersecting dips are directed toward the slope. It turns out that 18 planes are critical (out of 26) (**Figure 8**), while the probability of wedge failure reached 70% (**Figure 9**). Most of the time the reservoir is empty and free of passersby. The connection between rockfall and the danger to the dam is the presence of water in the reservoir at its highest level, which will dissipate after draining the reservoir water within approximately 36 hours. Thus, it can be concluded that the risks of the slope rocks can be disregarded.

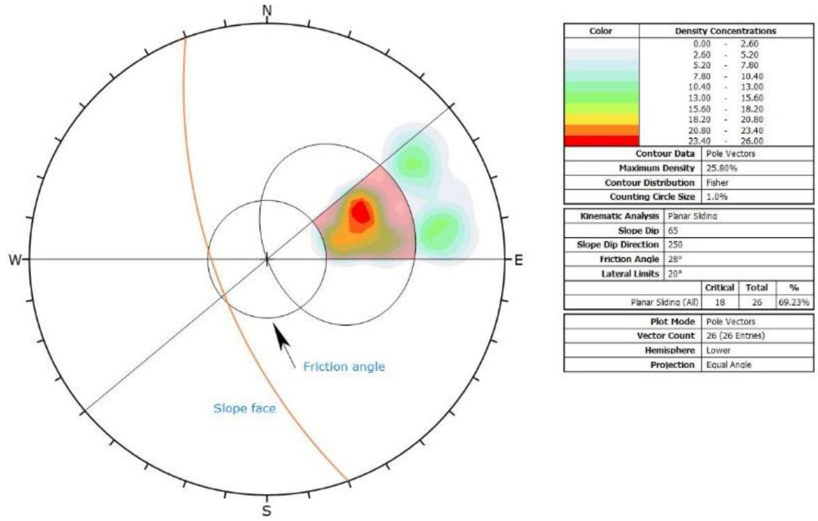

Figure 8. Kinematic analysis of potential plane failure in the northern rock slope adjacent to the reservoir. The stereo net plot identifies critical joint orientations that could generate planar instability under certain conditions.

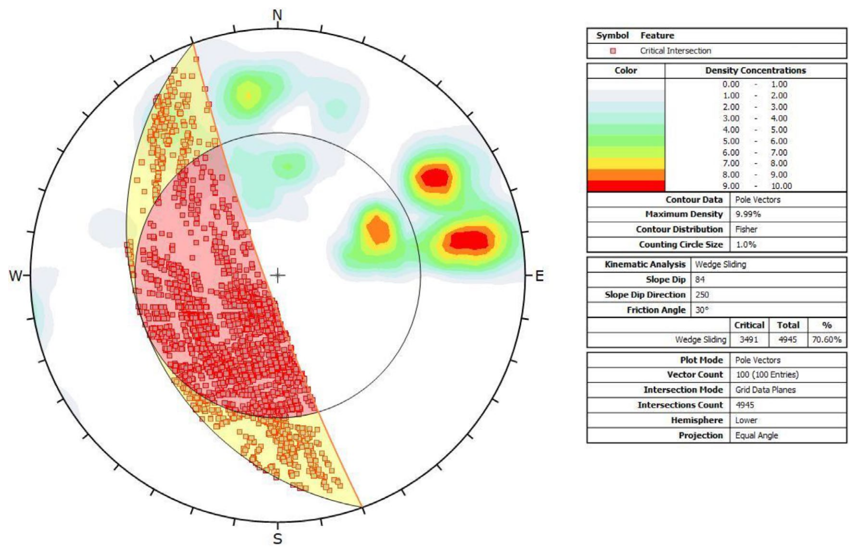

Figure 9. Kinematic analysis of potential wedge failure in the same slope, showing intersecting joint sets and their likelihood of forming unstable rock wedges. This analysis helps assess the probability of rockfall-induced wave generation in the reservoir.

7. Discussion

This dam falls among the most crucial attributes of the flood protection plan that was designed in Jeddah, a city that has long suffered fatal flash floods. SPT values of the soil at the base of the dam lie within an acceptable bearing capability. The static check of the dam accounts for the sliding, overturning, and seepage-related uplift conditions. Factor of safety (Fs) in overturning exceeds the minimum acceptable values; correspondingly, the Fs of the slope of the upstream face shows that the slope failure would not be under threat under current design in addition to loading conditions. These safety factors show acceptable design margins that are in accordance with the international standards of engineering, such as those by the United States Bureau of Reclamation (USBR) in addition to the United States Army Corps of Engineers (USACE), whose twin central functions in the United States are in the design, construction, and safety regulation of dams. Kinematic analysis by Dips 7 software reveals potential wedge failure, largely in areas of overlapping joint sets. While such failures are neither immediate, they would be a risk of generating water waves that may cause the dam crest to be overtopped in extreme events.

8. Conclusions

1) The large-capacity reservoir, in the study site, is sufficient to contain a major stormwater event with a 500-year return period. The calculated peak discharge for a 500-year rainstorm is 224 m^3/s, but this high value will not remain constant throughout the event; typically, half of that (112 m^3/s) is taken as the average. The reservoir will reach full capacity in eight hours and forty minutes, and the water level will rise to the freeboard without overtopping the dam crest.

2) The discharge capacity of the two pipes is 25.8 m^3/s under maximum head (8.5 m), and they are able to empty the entire reservoir water of a storm event of T500 in 36 hours (a day and a half). Seepage-induced instability was not performed because the water at its maximum level will last only 36 hours, and the dam upstream face is sealed by stones and concrete.

3) The calculated factor of safety for dam overturning, foundation, and dam face sliding is adequate and exceeds typical minimum requirements ($Fs \geq 1.3$ for overturning and sliding, $Fs \geq 1.5$ for bearing).

4) Although a windstorm may reach 100 km/h, its water waves would act away from the dam crest, posing no threat to the dam.

9. Recommendations

- Water seepage and pore water pressure in the dam body and its foundation must be monitored after major flood events.
- Dam soil internal erosion, piping, and the upstream concrete facing must be evaluated, especially under the dam toe, by reviewing seepage patterns.
- As a precaution, inclinometers may be installed, or survey benchmarks may be conducted to detect any lateral movement or settlement.

Acknowledgements

The author acknowledges the support and approval of the Saudi Geological Survey (SGS) for this research, conducted as part of the master's program at the Faculty of Earth Sciences, King Abdulaziz University. Special thanks are due to Professor Abdullah Sabtan for his guidance and continuous support.

Conflicts of Interest

The author declares no conflicts of interest regarding the publication of this paper.

References

[1] Moore, T.A. and Al-Rehaili, M.H. (1989) Geologic Map of the Makkah Quadrangle, Sheet 21D. Kingdom of Saudi Arabia. Saudi Arabian Directorate General of Minerals Resources, Jeddah, Map GM-107C, Scale 1:250.000.

[2] Al Shanti, A. (1966) Geologic Map of Wadi Fatima Iron Ore District (Scale Unknown). *Saudi Arabian Directorate General of Mineral Resources*, *Bulletin*, No. 2, 51 p.

[3] Brown, G.F., Jackson, R.O., Bogue, R.G. and Maclean, W.H. (1963) Geology of the Southern Hijaz Quadrangle, Kingdom of Saudi Arabia: Saudi Arabian Dir. Gen. Min. Res. Misc. Geologic Invest. Map 1-210A, 1:500,000 Scale.

[4] Nebert, K. (1974) Geologic Map of the Area North of Wadi Fatima- 1:50.000 -Plate. Institute of Applied Geology.

[5] Laurent, D., Daessle, M., Berton, Y. and Dehavi, M. (1973). Engineering Geological Map of Jeddah and Spot Information Map on Ground Conditions in Jeddah, Kingdom of Saudi Arabia: Saudi Arabia Dir. Gen. Min. Res. Geologic Map GM-8, Scale 1:100,000.

[6] Khogandi, M.E. (1989) Geology of the Jeddah City Area Open File Report. Ministry of Petroleum and Mineral Resources Directorate General of Mineral Resources, DGMR-OF-07-3, Kingdom of Saudi Arabia.

[7] Alqahtani, M.B. (1998) Engineering Geology of Greater Jeddah Metropolitan. Ph.D. Thesis, King Abdulaziz University.

[8] Yesubabu, V., Srinivas, C.V., Langodan, S. and Hoteit, I. (2015) Predicting Extreme Rainfall Events over Jeddah, Saudi Arabia: Impact of Data Assimilation with Conventional and Satellite Observations. *Quarterly Journal of the Royal Meteorological Society*, **142**, 327-348. https://doi.org/10.1002/qj.2654

[9] Alsaaq, F. and V.R., S. (2022) Extreme Wind Wave Climate off Jeddah Coast, the Red Sea. *Journal of Marine Science and Engineering*, **10**, Article 748. https://doi.org/10.3390/jmse10060748

[10] Geological Society of London (1977) The Description of Rock Mass for Engineering Purpose. Geological Society, Engineering Group, Working Party Report. *Quarterly Journal of Engineering Geology and Hydrogeology*, **10**, 355-389.

[11] IAEG (1976) Engineering Geological Maps. A Guide to their preparation. The UNESCO Press, 79.

[12] Federal Energy Regulatory Commission (2016) Engineering Guidelines for the Evaluation of Hydropower Projects: Chapter III Gravity Dams (Revision 3).

[13] U.S. Department of the Army and U.S. Army Corps of Engineers (2003) Engineering and Design: Slope Stability (EM 1110-2-1902). U.S. Army Corps of Engineers. https://www.publications.usace.army.mil

[14] Zhou, C., Shen, Z., Xu, L., Sun, Y., Zhang, W., Zhang, H., *et al.* (2023) Global Sensitivity Analysis Method for Embankment Dam Slope Stability Considering Seepage–stress Coupling under Changing Reservoir Water Levels. *Mathematics*, **11**, Article 2836. https://doi.org/10.3390/math11132836

[15] Fell, R., MacGregor, P., Stapledon, D., Bell, G. and Foster, M. (2014) Geotechnical Engineering of Dams. 2nd Edition, CRC Press.

[16] Das, B.M. and Sivakugan, N. (2016) Fundamentals of Geotechnical Engineering. 5th Edition, Cengage Learning.

[17] Terzaghi, K., Peck, R.B. and Mesri, G. (1996) Soil Mechanics in Engineering Practice.

3rd Edition, John Wiley & Sons.

[18] Piteau, D.R. (1972) Engineering Geology Considerations and Approach in Assessing the Stability of Rock Slopes. *Bulletin of the Association of Engineering Geologists*, **9**, 301-320.